

Histone hypomethylation is an indicator of epigenetic plasticity in quiescent lymphocytes

Jonathan Baxter^{1,4}, Stephan Sauer^{1,4},
Antoine Peters², Rosalind John¹,
Ruth Williams¹, Marie-Laure Caparros¹,
Katharine Arney¹, Arie Otte³, Thomas
Jenuwein², Matthias Merckenschlager¹
and Amanda G Fisher^{1,*}

¹Lymphocyte Development Group, MRC Clinical Sciences Centre, Imperial College School of Medicine, Hammersmith Hospital, London, UK, ²Research Institute of Molecular Pathology (IMP), Vienna Biocenter, Vienna, Austria and ³Swammerdam Institute for Life Sciences, University of Amsterdam, Amsterdam, Netherlands

Post-translational modifications of histone amino termini are thought to convey epigenetic information that extends the coding potential of DNA. In particular, histone lysine methylation has been implicated in conveying transcriptional memory and maintaining lineage fidelity. Here an analysis of histone lysine methylation in quiescent (G₀) and cycling lymphocytes showed that methylation of histone H3 at lysines 4 (H3K4), 9 (H3K9), 27 (H3K27) and histone H4 at lysine 20 is markedly reduced in resting B lymphocytes as compared with cycling cells. Quiescent B cells also lacked heterochromatin-associated HP1 β and Ikaros at pericentric chromatin and expressed low levels of Ezh2 and ESET histone methyl transferases (HMTases). Nuclei from resting B or T cells were approximately three times more efficiently reprogrammed in nuclear transfer assays than cells in which HMTase expression, histone methylation and HP1 β binding had been restored following mitotic stimulation. These results showing local and global changes in histone lysine methylation levels *in vivo* demonstrate that constitutive heterochromatin organization is modified in resting lymphocytes and suggest that histone hypomethylation is a useful indicator of epigenetic plasticity.

The EMBO Journal (2004) 23, 4462–4472. doi:10.1038/sj.emboj.7600414; Published online 28 October 2004

Subject Categories: chromatin & transcription; immunology
Keywords: histone; lymphocytes; methylation; reprogramming

Introduction

Covalent modifications to histone tails have been implicated in epigenetic inheritance based on observations that different

*Corresponding author. Lymphocyte Development Group, MRC Clinical Sciences Centre, Imperial College School of Medicine, Hammersmith Hospital, Du Cane Road, London W12 0NN, UK.
Tel.: +44 208 383 8238/39; Fax: +44 208 383 8338;
E-mail: amanda.fisher@csc.mrc.ac.uk

⁴These two authors contributed equally to this work

Received: 29 September 2003; accepted: 20 August 2004; published online: 28 October 2004

patterns of histone methylation and acetylation are predictably associated with distinct transcriptional states (Turner *et al*, 1992; Strahl *et al*, 1999; Turner, 2000; Jenuwein and Allis, 2001; Noma *et al*, 2001; Rice and Allis, 2001; Zhang and Reinberg, 2001; Berger, 2002). Histone modifications are postulated to both 'mark' the transcription state of genes and provide a self-templating mechanism to propagate chromatin status through DNA replication and mitosis (Jenuwein and Allis, 2001; Rice and Allis, 2001; Schreiber and Bernstein, 2002; Kurdستاني *et al*, 2004). Although histone acetylation and phosphorylation are reversible (Bannister *et al*, 2002), the energetic stability of histone lysine methylation (Byvoet *et al*, 1972; Duerre and Lee, 1974) may have a role in enhancing epigenetic stability, either by preserving heterochromatin structure or rendering histones less susceptible to additional modification (as discussed in Bannister *et al*, 2002).

Here we investigate the contribution of histone modifications to epigenetic memory by comparing the extent of histone lysine methylation between purified resting (G₀) and cycling lymphocytes. The rationale for this comparison lies with the capacity of quiescent lymphocytes to survive for extensive periods *in vivo*, and to re-enter the cell cycle only upon antigenic stimulation (Zhao *et al*, 1998). This implies that epigenetic information defining both the lineage and developmental stage of differentiated cells is actively retained in long-term quiescent cells. Mice lacking proteins that are essential for the clonal inheritance of gene activity, such as Polycomb group proteins (Kennison, 1995; Simon and Tamkun, 2002), show profound defects in lymphocyte proliferation in addition to homeotic transformations (van der Lugt *et al*, 1994; Akasaka *et al*, 1997; Core *et al*, 1997).

Previously, we have demonstrated that quiescent B lymphocytes lack some features of nuclear organization found in cycling cells, most noticeably a lack of spatial association of transcriptionally inactive genes and Ikaros proteins at pericentric heterochromatin (Brown *et al*, 1999). Here we show that chromatin composition differs dramatically between resting and cycling cells.

Results

Global changes in chromatin composition as lymphocytes enter the cell cycle

Noncycling splenic B cells (expressing B220) were isolated by CD43 depletion and stimulated with anti-IgM and anti-CD40 in the presence of interleukin-4 (IL-4). Under these conditions, *ex vivo* B cells express the activation marker CD69 within 24 h and begin DNA synthesis, as detected by BrdU incorporation, 48–72 h after stimulation (Figure 1A). The distribution of heterochromatin-associated proteins (Ikaros, HP1 β and CENP-A) in quiescent and activated cells was monitored by immunofluorescence (IF) and confocal microscopy (Figure 1B). In resting B cells, Ikaros protein was low or absent but increased following activation and relocated to

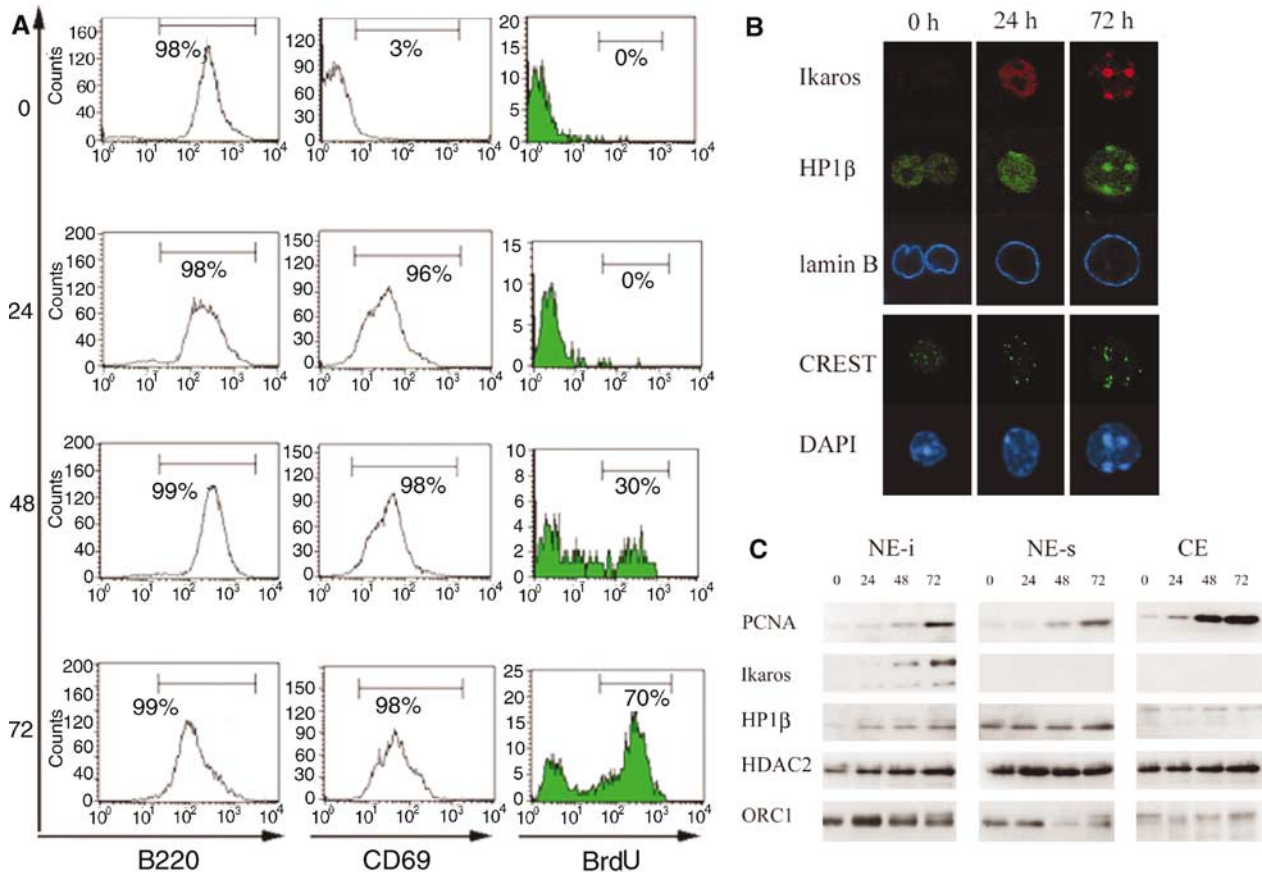


Figure 1 HP1 β and Ikaros proteins are upregulated and redistributed to constitutive heterochromatin in B lymphocytes following mitotic stimulation. (A) Kinetics of CD69 expression and BrdU incorporation by purified G₀ mouse B lymphocytes following mitotic stimulation with anti-IgM and CD40 antibodies. Cells were sampled 0, 24, 48 and 72 h poststimulation and the results show representative histograms of CD45RA (B220), CD69 and anti-BrdU labelling against cell number. (B) Upper panels: Representative confocal images of the nucleus of B lymphocytes simultaneously labelled with anti-Ikaros (red) and anti-HP1 β (M31, green) at 0, 24 and 72 h poststimulation in which the microscope and laser power settings were kept constant throughout so that the abundance and the relative distribution of proteins could be directly compared. The nuclear periphery of cells is outlined by lamin B labelling (blue). Lower panels: Confocal images of lymphocytes costained with CREST anti-sera (green) and DAPI (blue) for comparison. (C) Western blots confirming the abundance of specific proteins within cytoplasmic extracts (CE), DNase I-soluble nuclear extracts (NE-s) and DNase I-insoluble extracts (NE-i) at different times after B lymphocyte activation.

centromeric domains as reported previously (Brown *et al*, 1999). Low levels of HP1 β were detected in the nuclei of resting B cells. These increased slightly over 24 h, but HP1 β did not localize to DAPI-intense pericentric domains until 48–72 h after activation, concurrent with the lymphocytes commencing cell division. The kinetics of redistribution of Ikaros and HP1 β proteins were confirmed using antibodies specific for alternative regions of these proteins (not shown). This, and the demonstration that CREST antisera detect centromeres throughout B-cell activation (Figure 1B, lower panels), ruled out the possibility that epitope masking or restricted antibody accessibility accounts for a lack of Ikaros and HP1 β detection at constitutive heterochromatin in G₀ lymphocytes.

Global differences in chromatin composition were confirmed by Western blotting. For this analysis, nuclei from resting and activated cells were isolated by partial NP-40 lysis, subjected to DNase I digestion to yield soluble (NE-s) or insoluble (NE-i) nuclear fractions, and proteins separated by SDS-PAGE and analysed by Western blotting (Figure 1C). Controls included PCNA and ORC1 (used here to estimate the equivalence of protein loading). Low levels of PCNA were

detected in samples 48 h after stimulation, becoming more abundant in chromatin fractions after 72 h, consistent with most lymphocytes entering S-phase at this time. Ikaros proteins corresponding to the major isoforms present in lymphocytes (Hahm *et al*, 1994) were absent from G₀ samples (0 h), but accumulated in NE-i (chromatin-bound) fractions 48–72 h after stimulation. In contrast, HDAC2, a protein that interacts with many nuclear proteins including Ikaros (Kim *et al*, 1999), was abundant throughout B-cell activation. HP1 β protein was detected in the soluble chromatin compartment (NE-s) but showed increased levels within the insoluble (NE-i) fraction following activation, a result that is in agreement with the redistribution of HP1 β observed by IF.

Histone H3 lysine 9 methylation is reduced in quiescent B cells

The binding of HP1 β to pericentric heterochromatin is associated with the activity of Suv39h histone methyl transferases (HMTases), which are thought to generate a high-affinity binding site for HP1 β by catalysing the specific methylation of the N-terminus of histone H3 at lysine 9 (H3K9) (Bannister

et al, 2001; Lachner *et al*, 2001). We therefore examined the extent of H3K9 methylation in resting and cycling B cells with several anti-methyl H3K9 antibodies. Using an antibody to a branched peptide (α 4x(Me)₂H3K9) that recognizes a high density of H3K9 methylated positions (Peters *et al*, 2001), or an antibody raised to a linear H3K9 dimethyl peptide (UBI), we observed low or undetectable staining of quiescent B

lymphocytes (Figure 2A, top panel and data not shown). Although HP1 β can bind to either di- or trimethylated H3K9 *in vitro* (Bannister *et al*, 2001), *in vivo* the abundance of H3K9 trimethylation surrounding centromeres is thought to be responsible for HP1 β localizing to centromeric heterochromatin (Peters *et al*, 2003). Since the available 4x(Me)₂H3K9 and UBI linear (Me)₂H3K9 antibodies detect multiple H3

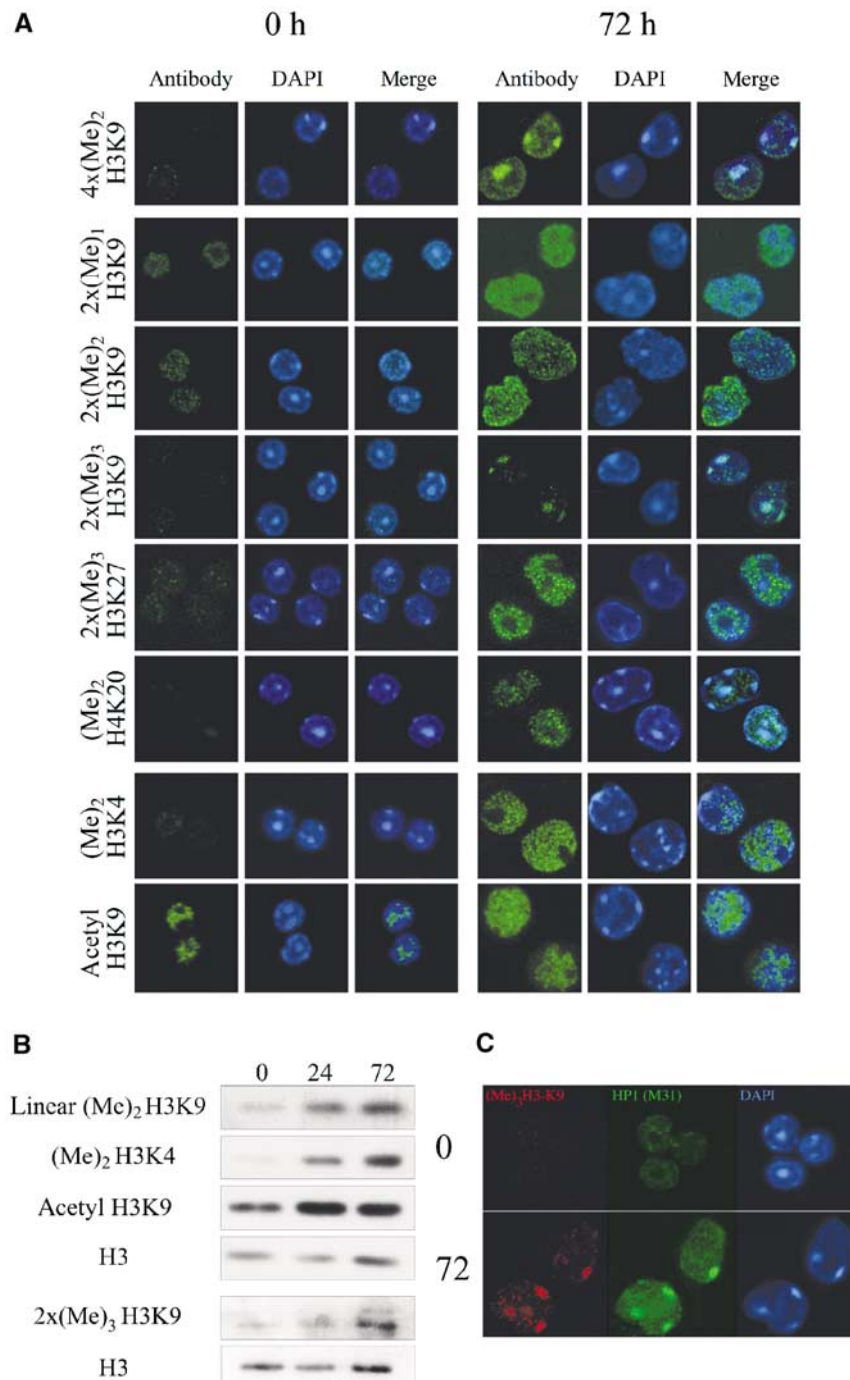


Figure 2 Histone methylation levels increase in B lymphocytes following mitotic stimulation. **(A)** IF images of the distribution of methylated H3K9, H3K27, H4K20 and H3K4 epitopes and acetylated H3K9 (shown in green), in quiescent (0 h) and cycling (72 h) B cells measured by IF relative to DAPI labelling (blue). **(B)** Relative abundance of modified histones estimated by Western blotting with appropriate antibodies using extracts prepared by either acid extraction of histones (top four panels) or whole-cells lysates (panels 5 and 6), harvested 0, 24 and 72 h after lymphocyte stimulation. H3 levels are shown for comparison. **(C)** Relative distribution of trimethyl H3K9 ((Me)₃H3K9, red), relative to HP1 β (M31, green) and DAPI labelling (blue) in resting (0h) and cycling (72 h) B cells.

methylation states, we used antibodies that were capable of recognizing and discriminating between mono- ($2x(\text{Me})_1\text{H3K9}$), di- ($2x(\text{Me})_2\text{H3K9}$) and trimethylated ($2x(\text{Me})_3\text{H3K9}$) states (Perez-Burgos *et al*, 2004). Using these highly specific reagents, we observed very low levels of H3K9 mono- and dimethylation in quiescent B cells, which consistently increased upon activation (Figure 2A and Supplementary Figure 1A).

H3K9 trimethylation was also low in most resting B cells (> 90%) and increased following activation (a comparison of labelling intensities is shown in Supplementary Figure 1A). H3K9 trimethylation was confined to discrete locations within the nucleus coincident with DAPI-bright, condensed chromatin domains (Figure 2A).

Interestingly, density fractionation of CD43-depleted populations showed that small 'resting' cells were completely devoid of H3K9 trimethylation, whereas some slightly larger cells (representing cells thought to have more recently exited cell cycle) displayed trimethylation at centromeric regions (Supplementary Figure 1B and C).

Confirmation that H3K9 di- and trimethylation levels were low in resting B-cell populations and increased upon activation was obtained by Western blotting (Figure 2B). Analysis of samples prepared 0, 24 and 48 h after activation confirmed an increase in di- and trimethylated H3K9 levels (Figure 2B) as compared to histone H3. Dual labelling of resting (0 h) and activated B cells (72 h) for trimethylated H3K9 (red, Figure 2C) and HP1 β (green, Figure 2C) showed that these proteins localized at constitutive heterochromatin (DAPI-intense blue, Figure 2C) in cycling lymphocytes but were either not detected or diffuse in resting cells, respectively. These data clearly demonstrate that the high levels of trimethylated H3K9 that normally decorate the pericentric heterochromatin of interphase and metaphase chromosomes are not in fact constitutive in B lymphocytes, but are acquired by cells upon entry into the cell cycle.

Increased H3 methylation in activated B lymphocytes

To examine whether other lysine residues of H3 were similarly undermethylated in resting B cells, antibodies that detect H3K4 methylation ($(\text{Me})_2\text{H3K4}$) or that are specific to trimethylated H3K27 ($2x(\text{Me})_3\text{H3K27}$) (Peters *et al*, 2003) were used. Labelling with these reagents was also low or undetectable in quiescent B cells but increased in cells preparing for division (Figure 2A), being routinely detected within 24 h of activation (Figure 2B, and data not shown). These changes did not appear to be restricted to H3 methylation since the levels of di- and trimethylated H4K20 were also substantially increased following activation (Figure 2A, and data not shown). Collectively, our data demonstrate that histone lysine methylation levels are globally reduced in resting B cells as compared to activated and cycling cells. We did not observe a dramatic reduction in H3K9 acetylation in resting cells (Figure 2A, lower panel, and Figure 2B) and only modest changes in acetylated H3K14 and H4 were seen (data not shown). Thus, although histone acetylation persists in quiescent B lymphocytes, lysine methylation appears to be poorly maintained.

The observation that methylated epitopes associated with transcriptionally permissive (H3K4) and repressive (H3K9 and H3K27) chromatin were both reduced in noncycling B cells suggests that hypomethylation may occur at a genome-

wide level. To assess directly the impact of these global changes at a local level, chromatin immunoprecipitation (ChIP) analyses were performed to compare histone methylation levels across the promoter regions of two expressed genes Pax5 and $\beta 2m$, the TdT gene (which is not expressed in mature B cells) and the major satellite repeat. We observed elevated levels of H3K4 methylation (and H3K9 acetylation) at the Pax5 and $\beta 2m$ promoter regions in cycling as compared with resting samples, consistent with the expression status of these genes and the increased transcription within activated B cells. Major satellite repeats (characteristic of pericentric regions) showed very low levels of acetylated H3K9 and methylated H3K4 regardless of cell cycle status. In contrast, H3K9 methylation of major satellite repeats increased 7.5-fold upon activation. In these experiments, we can exclude potential differences in DNA recovery from resting and cycling samples, as individual samples 'spiked' with chromatin from *Drosophila* S2 cells before immunoprecipitation showed similar levels of methylated K9, K4 and acetylated K9 at two *Drosophila* loci DNA (see Supplementary Figure 2). In the case of the TdT gene (Su *et al*, 2004), we observed a more complex profile. Activated B cells showed a seven- to eight-fold enrichment of methylated H3K9 and H3K4 compared to resting B cells while H3K9 acetylation levels remained fairly constant (< 2-fold increase). Overall, these data demonstrate that levels of histone lysine methylation are consistently increased in primary B cells following mitotic stimulation. This occurs at the promoters of genes that are required to maintain B-cell identity (such as Pax5), that are specifically silenced during B-cell development (such as TdT), as well as regions of the genome that are normally actively expressed ($\beta 2m$) or repressed (major satellite).

To determine whether activation-induced increases in H3K9 methylation are dependent on Suv39h, we examined B cells from mice that were double deficient for the *Suv39h1* and *Suv39h2* HMTases (Suv39h dn; Figure 3). Resting Suv39h dn B cells had low levels of H3K9 methylation and showed a significant increase in euchromatic H3K9 methylation upon activation (72 h). In contrast to normal cells, no enrichment of H3K9 methylation or HP1 β accumulation at pericentric heterochromatin was observed following activation (Figure 4) (Peters *et al*, 2001). Ikaros protein remained associated with pericentric heterochromatin in Suv39h dn lymphocytes (Figure 4, lower right-hand panel), demonstrating that Ikaros recognizes pericentric regions independently of HP1, consistent with Ikaros binding directly to repetitive DNA sequences that flank centromeres (Cobb *et al*, 2000).

Increased reprogramming potential of quiescent T and B lymphocytes

Quiescent T lymphocytes isolated directly from mouse lymph nodes also showed reduced levels of histone methylation compared to cycling cells (see Supplementary Figure 3). In particular, H3K9 methylation (as recognized by HP1 β , green) was low in *ex vivo* T cells (identified by TCR expression, red), whereas after activation with immobilized anti-TCR β and CD28 antibody, HP1 β -labelling was intense and focused at DAPI-bright regions. These data argue that diminished H3K9 methylation is a feature of noncycling T as well as B lymphocytes.

One possible consequence of reduced histone lysine methylation might be to effectively 'loosen' the epigenetic

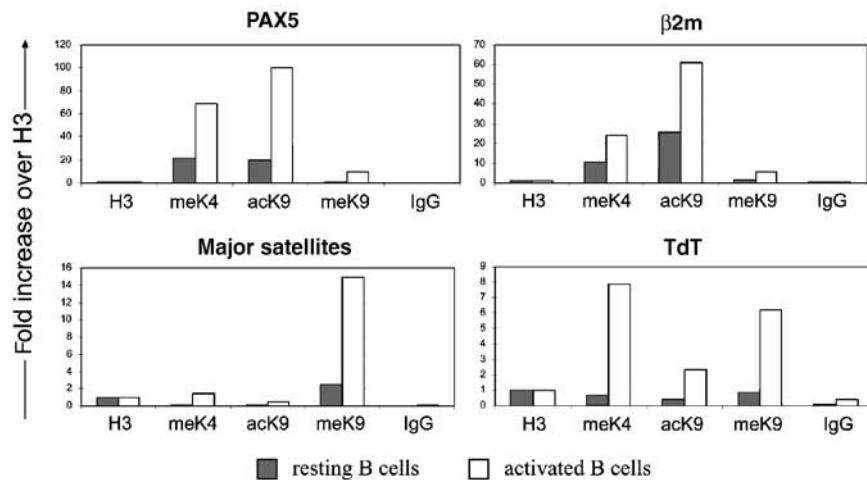


Figure 3 ChIP analysis of histone modifications at specific loci. Data represent mean values of three independent ChIP experiments in which levels of H3K4 and H3K9 methylation and H3K9 acetylation at the promoters of Pax5, $\beta 2M$ and TdT genes and across major satellite repeats were determined relative to H3. Histones were immunoprecipitated from both resting (grey) and activated (white) B-cell samples, and rabbit antisera to histone H3 C-terminus and to mouse IgG were used as 'input' and negative controls in each immunoprecipitation, respectively.

code and thereby enhance the cellular plasticity of resting cells. This could, in principle, offer an explanation for long-standing claims that some resting (or serum-starved) populations of cells are more efficiently reprogrammed than activated cells (Gurdon *et al*, 1975; Wilmut *et al*, 1997; Kikyo and Wolffe, 2000). To test whether resting lymphocytes were indeed reprogrammed at a higher frequency than activated cells, we performed nuclear transfer experiments using fertilized embryos as recipients. This allows the potential of different donor nuclei to be assessed in a context where their contribution to embryonic development is not required (Modlinski, 1978). As an indicator of plasticity, we analysed the reactivation of an EGFP transgene (Hadjantonakis *et al*, 1998; Eggen *et al*, 2000) that is normally inactive in lymphocytes, following transfer of lymphocyte nuclei into one-cell embryos. As illustrated in Figure 5A, transgenic mice expressed the EGFP transgene in most tissues including kidney (K) and liver (L). Transgene expression was low in the thymus (T) and EGFP mRNA was not detected in purified splenic B cells (resting B⁰, activated B⁷²) or lymph node T cells (not shown). Lymphocyte nuclei from EGFP male mice were injected into nontransgenic fertilized embryos and the frequency of GFP re-expression was monitored 3–4 days later (exemplified in Figure 5B). Approximately three times as many fertilized embryos re-expressed GFP when injected with resting B cell nuclei as those injected with 48 or 72 h activated B cells (Figure 5C). Similarly, nuclear transfer experiments using lymph node T cells from EGFP transgenic male mice (as donors) showed that three times more embryos re-expressed GFP when injected with nuclei from resting T cells than 72 h activated T cells. Previous reports showing the enhanced reprogramming performance of resting cell populations have suggested that cycling populations are compromised because mitotic and S-phase cells are not well coordinated with the recipient cell cycle phase and cannot maintain ploidy (reviewed in Campbell and Alberio, 2003). To dissociate the impact of H3 hypomethylation from these cell cycle events, we assessed the reprogramming potential of nuclei isolated 24 h after activation, when histone remethyla-

tion was evident (Figure 2B, middle column) but before cells have started to replicate DNA (Figure 1A). Interestingly, these nuclei were remarkably resistant to reprogramming (0 of 85 embryos; Figure 5C), whereas control cells incubated for 24 h in IL-4 alone (that did not remethylate) showed a similar reprogramming capacity as *ex vivo* resting B lymphocytes. These data show that not only is histone lysine hypomethylation an important predictor of enhanced cell plasticity but also that elevated reprogramming potential is an intrinsic feature of resting lymphocytes.

Histone hypomethylation in G₀ Kupffer cells in liver

To determine whether quiescent cells other than lymphocytes have reduced levels of histone methylation, we examined noncycling populations within the liver. Liver sections labelled with α 4x(Me)₂H3K9 antibodies showed evidence of two distinct cell subsets. The majority of cells, including those with large nuclei (12–16 μ m diameter), expressed high levels of H3K9 methylation. A second population with smaller nuclei (8–9 μ m diameter) apparently lacked H3K9 methylation (Figure 6A). The relative abundance of the two cell types was consistent with the larger cells being hepatocytes and the smaller cells being Kupffer cells. To confirm this, we prepared single-cell suspensions of murine liver by collagenase treatment (Seglen, 1976), and identified Kupffer cells on the basis of expression of the leucocyte-specific membrane protein CD45. As shown in Figure 6B, Kupffer cells expressing surface CD45 (identified by biotinylated anti-CD45 and FITC-avidin, green) were conveniently discriminated from larger hepatocytes in which endogenous biotin was restricted to the cytoplasm. Colabelling of liver cell suspensions with α 4x(Me)₂H3K9 antibodies confirmed that the hepatocytes showed high levels of H3K9 methylation, while no labelling was apparent in the nuclei of *ex vivo* Kupffer cells. Methylated H3K4 was also detected in hepatocytes but not in Kupffer cells (Figure 6B, right panel). Consistent with previous experiments in lymphocytes, histone lysine hypomethylation was rapidly reversed by mitotic stimulation, as indicated by increased H3K9 methylation

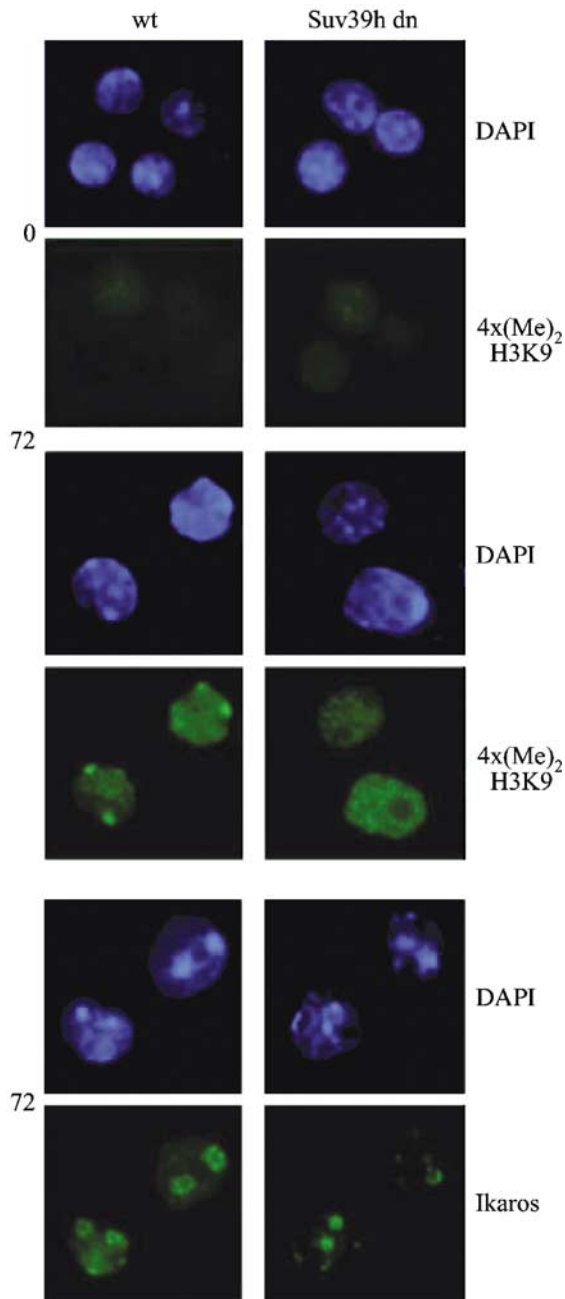


Figure 4 Suv39h contributes to upregulation of H3K9 methylation at pericentric heterochromatin but is not required for Ikaros recruitment. Methylated H3K9 in resting (0 h) and cycling (72 h) samples is shown (4x(Me)₂H3K9 labelling, green) relative to DAPI-intense regions (blue) in B cells isolated from normal male (wild type) and Suv39h-deficient (Suv39dn) mice. The distribution of Ikaros proteins (green) in the nucleus of cycling B lymphocytes was not affected by the absence of Suv39h HMTases, as shown in the lower panels.

(red) in CD45-positive Kupffer cells (green) following overnight culture in the presence of GM-SCF, CSF and interleukin 3 (IL-3) (Figure 6C). These data confirm that H3 hypomethylation is reversed upon re-entry into the cell cycle.

Reversing histone lysine methylation

Several reports have shown that histones can be replaced in both a replication-dependent and replication-independent manner (Wu *et al*, 1982; Pina and Suau, 1987; Bannister

et al, 2002), with noncycling cells accumulating the variant histone H3.3 (Pina and Suau, 1987; Lennox and Cohen, 1988). H3.3 predominance has been documented in chromatin from liver, brain, kidney and neurons (Bonner *et al*, 1980; Bosch and Suau, 1995), and in lymphocytes the relative abundance of H3.3 has been shown to reflect directly the length of time in quiescence (Wu *et al*, 1983). More recently, replacement of H3.1 by H3.3 has been shown at specific loci where exchange appears to be driven by active transcription (Ahmad and Henikoff, 2002). On the basis of this information, a two-step mechanism can be proposed to explain how histone lysine methylation levels decline as lymphocytes withdraw from the cell cycle: the gradual exchange and accumulation of H3.3 in noncycling cells (histone replacement) coupled with reduced HMTase activity. Genome-wide changes in histone methylation levels in response to cell activation could result from structural changes rendering the chromatin of activated lymphocytes more accessible to various enzymes responsible for histone methylation, or could be due to a selective upregulation of HMTases in cycling cells. To investigate these possibilities, we compared the sensitivity of nuclear extracts from resting (R) and activated (A) primary B cells to increasing concentrations of micrococcal nuclease (Figure 7A) and also examined the distribution of Ezh2 and ESET HMTases following activation (Figure 7B). The nuclease sensitivity of activated B cells was broadly similar to that of a control pre-B-cell line (C), whereas samples prepared from resting B cells showed a two- to three-fold reduced sensitivity. In addition, IF and Western blotting showed that ESET and Ezh2 HMTases were low or undetectable in most quiescent B lymphocytes (Figure 7B). Following lymphocyte activation, ESET, Ezh2 and Bmi1 (a component of the Polycomb Repressor Complex 1) were all upregulated, whereas Eed levels remained relatively unchanged. These data show that chromatin accessibility, HMTase levels and the distribution of structural components of heterochromatin (such as HP1 β) are globally modified upon mitotic stimulation demonstrating that 'constitutive' heterochromatin is surprisingly dynamic *in vivo*.

Discussion

Using antisera that recognize specific histone methylation states, we provide evidence for histone lysine hypomethylation in G₀ B lymphocytes, T lymphocytes and Kupffer cells. Following mitotic stimulation, methylation of H3 at lysines 4, 9, 27 (and H4 at lysine 20) is reinstated in lymphocytes concurrent with an upregulation and redistribution of several chromatin modifier proteins. During this time, the nuclear volume of lymphocytes increases approximately four- to five-fold (Zhao *et al*, 1998) and chromatin accessibility to micrococcal nuclease digestion is also increased. We observe that trimethylation of H3K9, commonly regarded as a functional 'hallmark' of constitutive heterochromatin, is substantially upregulated in cells following mitogenic stimulation.

The observed absence of histone lysine methylation in these G₀ populations is unlikely to be due to 'masking' and subsequent 'unmasking' of methyl epitopes following activation for several reasons. First, antisera to different molecular epitopes show a consistent reduction in histone methylation

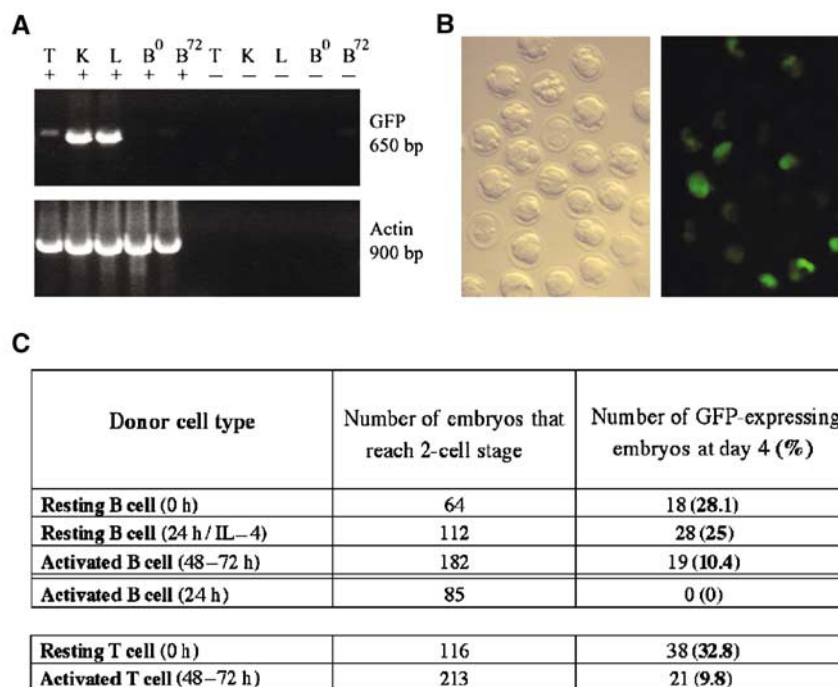


Figure 5 Activation of a silent EGFP transgene is more efficient using G_0 lymphocytes as donors for nuclear transfer. Mice carrying an EGFP transgene express EGFP from the morula stage in early mouse embryos (not shown) and in many adult tissues, but the transgene is silent in both resting and active B cells as shown by flow cytometry (not shown) and RT-PCR. RT-PCR analysis of EGFP expression in thymus (T), kidney (K), liver (L) and purified resting (B^0) and activated (B^{72}) splenic B cells is shown in (A) where the addition (+) or lack (-) of reverse transcriptase in each reaction is indicated. (B) Following transfer of donor lymphocyte nuclei into embryos and their *in vitro* development, some embryos were GFP fluorescent (right panel—shown in bright field in the left panel) indicating variable re-expression of the EGFP transgene in tetraploid embryos. (C) Summary of the re-expression of EGFP transgene in tetraploid embryos generated by nuclear transfer using resting (0 h) or active B (24, 48–72 h) and T cells as donors. Here, consistently three times as many embryos showed detectable GFP expression after transfer with resting cell nuclei as compared with 48–72 h activated cell nuclei in results derived from 14 experiments.

as judged by IF. Second, these observations were confirmed by Western blotting analyses where steric masking of epitopes is not an issue. Third, reduced H3 methyl-lysine labeling of resting cells is observed even within presumed euchromatin (methyl H3K4) domains and at actively transcribed genes (such as $\beta 2$ microglobulin).

The finding that histone lysine methylation declines in long-term quiescent B cells, whereas histone acetylation is clearly observable, is intriguing and unexpected. An explanation for this could be that the low-level transcription of active genes in G_0 lymphocytes is sufficient to maintain histone acetylation of the lymphocyte genome. In contrast, high levels of histone lysine methylation may only be required when overall gene activity is increased (e.g., following mitotic stimulation) to reaffirm the epigenetic state of a gene prior to DNA synthesis.

Current views on how the histone code might be ‘read’ have suggested that the quality and density of distinct histone tail modifications could predict transcriptional potential. Where changes in histone methylation levels have been shown to occur, they have indeed been linked to alterations in gene expression (Janicki *et al*, 2004; Mutskov and Felsenfeld, 2004; Su *et al*, 2004). Here we show that the relative abundance of histone lysine methylation also differs dramatically between resting and cycling populations of lymphocytes, although here the overall gene expression profile remains consistent with B-cell identity (Hoffmann *et al*, 2002). These global changes in histone methylation

levels are also reflected at the level of individual genes. ChIP analysis revealed a marked increase in methylated H3K9 and H3K4 in the promoter regions of Pax5, $\beta 2m$ and TdT genes upon cell activation, and a seven- to eight-fold upregulation of H3K9 methylation at major satellite regions. These do not necessarily negate the concept that histone lysine methylation contributes to cellular memory since even relatively low levels of these modifications could still be sufficient to ‘mark’ active or inactive chromatin domains in quiescent cells.

In summary, we show here that in some cell types exit from the cell cycle is accompanied by a substantial reduction in histone lysine methylation levels. Quiescent lymphocytes display a global reduction in histone lysine methylation and modifications in constitutive heterochromatin organization. Thus conventional hallmarks, such as trimethylation of H3K9, Ikaros association and HP1 binding, are not apparent in resting cells, but are reinstated dynamically in response to mitotic stimulation. Resting lymphocytes were also shown to be more successfully reprogrammed than either cycling cells or lymphocytes in which histone methylation was transiently restored. These results caution that among non-cycling cells, which comprise a substantial proportion of most organisms, reduced histone methylation levels do not simply reflect transcriptional competence. Rather, histone hypomethylation provides a novel indicator of an enhanced epigenetic plasticity of resting cell populations such as lymphocytes.

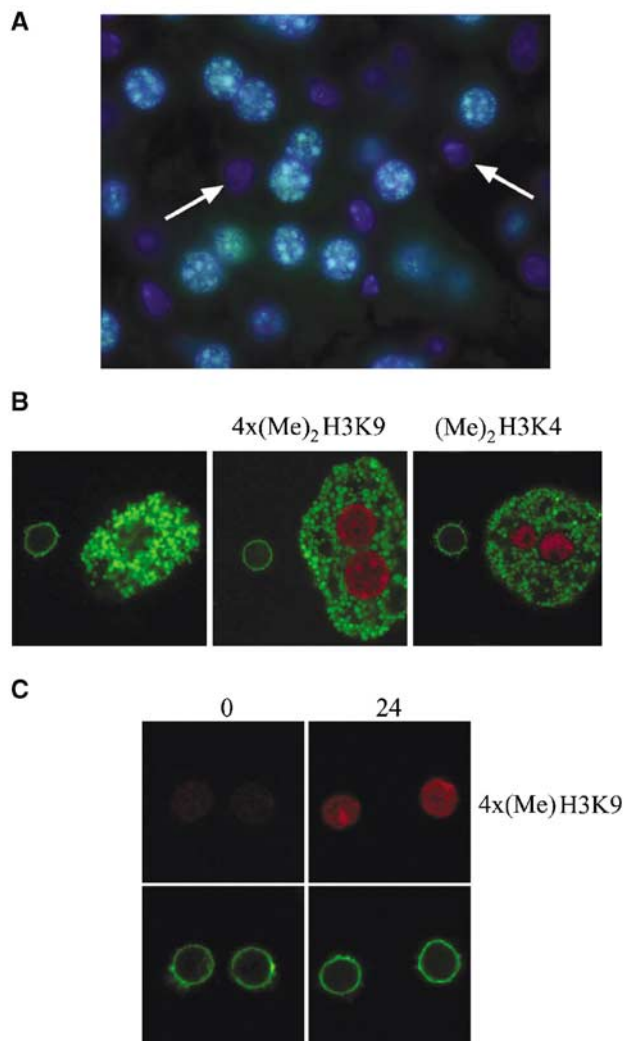


Figure 6 Histone lysine hypomethylation of Kupffer cells in liver. (A) In mouse adult liver sections labelled with α 4x(Me)₂H3K9 (green) and DAPI (blue), a population of cells lacking methylated H3K9 is seen (arrowed). (B) Labelling of isolated liver cell suspensions with biotinylated CD45 antibody revealed with avidin-FITC (green) either alone (left) or costaining with antibody to methylated H3K9 (α 4x(Me)₂H3K9, red) or methylated H3K4 ((Me)₂H3K4, red). (C) α 4x(Me)₂H3K9 labelling (red) of freshly isolated Kupffer cells (0 h) and following mitotic stimulation (24 h in GM-CSF and IL-3), where Kupffer cells were identified by labelling with anti-CD45 (green).

Materials and methods

Purification and activation of resting B lymphocytes from spleen

Normal resting B cells were prepared as described previously (Brown *et al*, 1999). For details, see Supplementary material. B-cell activation was induced by culturing cells in IMDM media containing 10% fetal bovine serum (Sigma) and antibiotics and 20 μ g/ml purified anti-CD40 (monoclonal antibody FGK45), 10 μ g/ml purified anti-IgM (monoclonal antibody H3074) and 2% IL-4 containing supernatant (from a T-helper cell line). Fluorescein-labelled antibodies to B220 and CD69 (BD Pharmingen) were used for FACS analysis to verify the phenotype and activation status of cells. Percoll purification of cells was carried out as described elsewhere (Ratcliffe and Julius, 1982).

BrdU incorporation studies were performed using *ex vivo* resting mature B cells. Cells were cultured in media containing 50 μ M BrdU with either IL-4 for 24 h (for unstimulated cells) or following

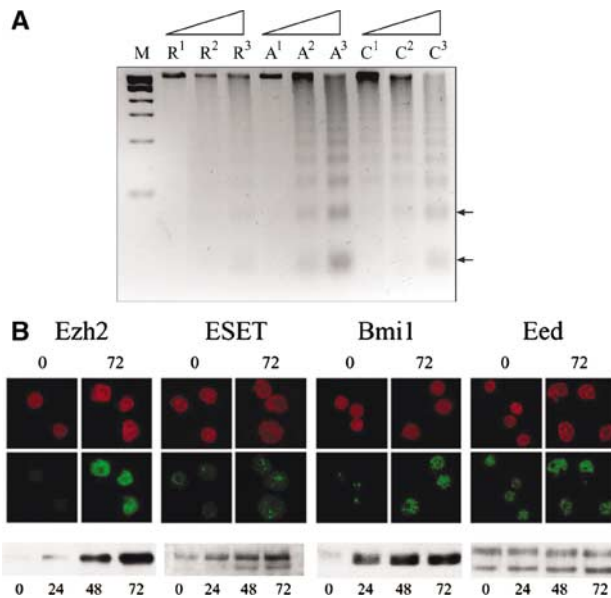


Figure 7 Changes in chromatin accessibility and HMTase distribution accompany B-cell activation. (A) Micrococcal nuclease accessibility assays performed on nuclear extracts of resting (R) and activated (A) B lymphocytes and a control pre-B-cell line (C). Chromatin equivalent to 10 μ g of genomic DNA was subjected to increasing MNase digestion: 5 U, 7.5 U MNase for 10 min (R¹, R²) or with 7.5 U MNase for 15 min (R³). Di- and trinucleosome DNA fragments (indicated by arrows) were seen as a result of increased digest duration and enzyme concentration in the extracts of activated and control cells and to a reduced extent in resting cells. (B) Representative confocal images showing the distribution of Ezh2, Eed, Bmi1 and ESET proteins (depicted in green) relative to PI-labelled DNA dense regions (red) in the nuclei of quiescent (0 h) and cycling (72 h) B lymphocytes. The relative abundance of these proteins in the nuclear extracts of B cells harvested 0, 24, 48 and 72 h after activation was assessed by Western blotting as shown in the lower panels.

activation using anti-IgM, anti-CD40 and IL-4 as described above. BrdU incorporation was revealed as previously described (Huesmann *et al*, 1991), and is described in detail in Supplementary material.

Preparation of liver sections and cell suspensions

Liver sections were prepared and labelled as outlined elsewhere (Czvitkovich *et al*, 2001). Liver cells were prepared using a two-step procedure described previously (Seglen, 1976) with minor modifications. For details, see Supplementary material. Freshly isolated Kupffer cells were activated by overnight incubation in IMDM media containing 10% fetal bovine serum, antibiotics, 5% WEHI-3B supernatant (containing IL-3), 10 ng/ml murine GM-SCF and 10 ng/ml murine CSF-1.

Antibody labelling and fluorescence microscopy

Antibodies used for IF and Western blot studies were rabbit anti-N- and C-terminus Ikaros (Hahm *et al*, 1998), rat anti-M31 (HP1 β , Serotec) (Wreggett *et al*, 1994), goat anti-lamin B (Santa Cruz), human CREST autoimmune sera and rabbit antisera to α -4-dimeth H3-K9, α -2x-monometh H3-K9, α -2x-dimeth H3-K9, α -2x-trimeth H3-K9, α -2x-trimeth H3-K27 (Peters *et al*, 2001, 2003; Perez-Burgos *et al*, 2004), α -dimeth H3-K9, α -dimeth H3-K4 (UBI), acetyl H3-K9, acetyl H3-K14 (UBI), pan-acetyl H4 (Serotec), Ezh2 (Sewalt *et al*, 1998), EED (van der Vlag and Otte, 1999), Bmi1 (Gunster *et al*, 1997) and ESET (Yang *et al*, 2002). Additional antibodies used as controls in these analyses were anti-HP1 β (Euromedex), anti-ORC1 (Serotec) and anti-PCNA (Sigma). IF staining of proteins was carried out by standard methods described in Supplementary material. IF staining of histone modifications was performed as described (Peters *et al*, 2001) with minor modifications described in Supplementary material. Samples were mounted in Vectashield

supplemented with DAPI and visualized either by confocal microscopy using a TCS-SP1 (Leica Microsystems) or using an Axioplan 2E microscope (Zeiss), Metamorph 4.0 software and images were processed using Adobe Photoshop 6.0. In comparisons between quiescent and cycling cells, microscope settings and laser power were kept constant, so that the relative abundance and distribution of labelled proteins could be directly compared.

Preparation of nuclear extracts from ex vivo B lymphocytes and Western blot analyses

For preparing NE-i, NE-s and cytoplasmic extracts (CE), B cells were washed in ice-cold PBS, centrifuged at 600 g for 4 min in a chilled centrifuge (4°C) and resuspended in ice-cold nuclei lysis buffer (10 mM Pipes, pH 6.8, 100 mM NaCl, 300 mM sucrose, 3 mM MgCl₂, 1 mM EGTA, supplemented with protease inhibitor cocktail and phosphatase cocktail (Sigma) and 1 mM DTT). Lysis buffer containing 0.75% NP-40 was added dropwise until the concentration of NP-40 reached 0.15% and then left on ice for 2 min before centrifugation at 400 g for 2 min. The cytoplasmic fraction (supernatant) was collected and the remaining nuclei were washed once in lysis buffer and centrifuged again as described previously. Chromatin was solubilized by DNA digestion with 1 mg/ml of RNase-free DNase I (Sigma) in lysis buffer for 30 min at 30°C. (NH₄)₂SO₄ was added from a 1 M stock solution in lysis buffer to a final concentration of 0.25 M. After 5 min on ice, samples were pelleted by centrifuging at 1500 g for 3 min and DNase I-soluble material was collected. The pellet containing DNase I-insoluble material was then solubilized in urea buffer (8 M urea, 0.1 M NaH₂PO₄ and 0.01 M Tris-HCl pH 8.0) and the protein extracts were quantified and stored at -70°C.

Histone proteins were isolated from whole cells by acid extraction. A total of 1×10^7 B cells were pelleted, resuspended in 1 ml PBS (4°C), centrifuged (500 g for 5 min) and the supernatant was removed. Cell pellets were resuspended in 180 µl of ice-cold lysis buffer (10 mM HEPES pH 7.9, 1.5 mM MgCl₂, 10 mM KCl, 0.5 mM DTT and 1.5 mM PMSF), 20 µl of 2 M HCl added and incubated on ice for 30 min. Following acid lysis, the solution was centrifuged at 11000 g for 10 min at 4°C, the supernatant of acid-soluble proteins collected and sequentially dialysed against 0.1 M acetic acid (twice for 1 h) and water (1 h, 3 h and overnight). The protein solution was quantified and stored at -70°C. Whole-cell extracts were prepared by direct lysis of cells in SDS loading buffer. Western blotting of protein extracts was carried out as described previously (Brown *et al*, 1999).

Chromatin immunoprecipitation assays

Approximately 10⁸ primary B cells and *Drosophila melanogaster* Schneider 2 (S2) cells were mixed in a 5:1 ratio and prepared for ChIP analysis as described (Peters *et al*, 2003) with minor modifications. A 150 µg portion of chromatin was subjected to immunoprecipitation with 5 µl of rabbit antibody (1 mg/ml α-4x-dimethyl H3K9, -dimethyl H3K4, -acetyl H3K9 and -mouse IgG) or 0.5 µl of H3-C terminal antibody (Abcam, ab1791), which served as an input control. After elution of immune complexes, DNA was resuspended in 40 µl TE and 2 µl was used per quantitative PCR (qPCR) reaction.

Quantitative PCR analysis

qPCR analysis was carried out using Sybr-Green PCR Mastermix (Applied Biosystems) on an Opticon™ DNA engine (MJ Research

Inc.) using Opticon Monitor 1.04 software (MJ Research Inc., 2000–2002), running the following program: 94°C for 8 min, then 40 cycles of 94°C for 20 s, 55°C for 20 s, 72°C for 30 s, followed by plate-read. For primer sequences, see Materials and methods of Supplementary material.

Reprogramming assays, nuclear transfer and EGFP transgenic mice

Somatic nuclei can be reprogrammed by nuclear transfer into enucleated oocytes as originally described by Wakayama *et al* (1998). Although approximately 20–40% of renucleated oocytes develop to the blastocyst stage, in most cases less than 1% result in live-born animals, suggesting that complete reprogramming is a rare event (reviewed in Yanagimachi, 2002). Reprogramming can also be achieved by nuclear transfer into fertilized mouse eggs (Modlinski, 1978). Although this generates tetraploidy in the resulting embryos, the technique is more robust and allows an assessment of the differences in reprogramming potential of multiple cell types. In our studies, mice carrying an EGFP transgene (Hadjantonakis *et al*, 1998; Eggan *et al*, 2000) were used as a source of donor cells (a kind gift from Dr A Nagy). The EGFP transgene is expressed from the morula stage onwards and in most tissues, but is silent in both resting and cycling lymphocytes (as determined by flow cytometry detection of GFP protein or RT-PCR analysis of EGFP mRNA). For further details, see Supplementary material.

Chromatin accessibility assay

Nuclei from resting, activated primary B cells, and from the pre-B-cell line B3, were isolated and prepared as previously. The pellet was washed in ice-cold lysis buffer (10 mM Pipes pH 6.8, 100 mM NaCl, 300 mM sucrose, 3 mM MgCl₂, 1 mM EGTA, 1 mM DTT and protease inhibitors (Roche)) and resuspended in 400 µl of nuclear buffer (20 mM Tris-HCl pH 7.5, 70 mM NaCl, 20 mM KCl, 5 mM MgCl₂, 3 mM CaCl₂ and protease inhibitors). The DNA concentration was determined by spectrophotometric analysis (OD₂₆₀) and 10 µg of DNA was subjected to digestion with micrococcal nuclease (MNase, Sigma) before the reaction was stopped with EDTA and EGTA. Equal amounts of supernatant were run on a 2% agarose gel to estimate digestion efficiency.

Supplementary data

Supplementary data are available at *The EMBO Journal* Online.

Acknowledgements

We thank Professors N Brockdorff, B Turner, J Blow and Drs J Mermoud and S Barton for helpful discussions and advice and Mr G Reed for help with photography. We thank Dr Y Zhang for the anti-ESET antibody. This study was supported by the Medical Research Council UK and the Institute of Molecular Pathology through Boehringer Ingelheim, a Marie Curie Industry Host Fellowship (AP), and grants from the National Institutes of Health (JB and KA), the BBSRC (RW), an MRC-T Development Gap Award (RJ and M-LC), the Vienna Economy Promotion Fund and European Union Intellectual Property Network and Austrian GEN-AU initiative (TJ).

References

- Ahmad K, Henikoff S (2002) The histone variant H3.3 marks active chromatin by replication-independent nucleosome assembly. *Mol Cell* **9**: 1191–1200
- Akasaka T, Tsuji K, Kawahira H, Kanno M, Harigaya K, Hu L, Ebihara Y, Nakahata T, Tetsu O, Taniguchi M, Koseki H (1997) The role of mel-18, a mammalian Polycomb group gene, during IL-7-dependent proliferation of lymphocyte precursors. *Immunity* **7**: 135–146
- Bannister AJ, Schneider R, Kouzarides T (2002) Histone methylation: dynamic or static? *Cell* **109**: 801–806
- Bannister AJ, Zegerman P, Partridge JF, Miska EA, Thomas JO, Allshire RC, Kouzarides T (2001) Selective recognition of methylated lysine 9 on histone H3 by the HP1 chromo domain. *Nature* **410**: 120–124
- Berger SL (2002) Histone modifications in transcriptional regulation. *Curr Opin Genet Dev* **12**: 142–148
- Bonner WM, West MH, Stedman JD (1980) Two-dimensional gel analysis of histones in acid extracts of nuclei, cells, and tissues. *Eur J Biochem* **109**: 17–23
- Bosch A, Suau P (1995) Changes in core histone variant composition in differentiating neurons: the roles of differential turnover and synthesis rates. *Eur J Cell Biol* **68**: 220–225

- Brown KE, Baxter J, Graf D, Merckenschlager M, Fisher AG (1999) Dynamic repositioning of genes in the nucleus of lymphocytes preparing for cell division. *Mol Cell* **3**: 207–217
- Byvoet P, Shepherd GR, Hardin JM, Noland BJ (1972) The distribution and turnover of labeled methyl groups in histone fractions of cultured mammalian cells. *Arch Biochem Biophys* **148**: 558–567
- Campbell KH, Alberio R (2003) Reprogramming the genome: role of the cell cycle. *Reprod Suppl* **61**: 477–494
- Cobb BS, Morales-Alcelay S, Kleiger G, Brown KE, Fisher AG, Smale ST (2000) Targeting of Ikaros to pericentromeric heterochromatin by direct DNA binding. *Genes Dev* **14**: 2146–2160
- Core N, Bel S, Gaunt SJ, Aurrand-Lions M, Pearce J, Fisher A, Djabali M (1997) Altered cellular proliferation and mesoderm patterning in Polycomb-M33-deficient mice. *Development* **124**: 721–729
- Czvitkovich S, Sauer S, Peters AH, Deiner E, Wolf A, Laible G, Opravil S, Beug H, Jenuwein T (2001) Over-expression of the SUV39H1 histone methyltransferase induces altered proliferation and differentiation in transgenic mice. *Mech Dev* **107**: 141–153
- Duerre JA, Lee CT (1974) *In vivo* methylation and turnover of rat brain histones. *J Neurochem* **23**: 541–547
- Eggan K, Akutsu H, Hochedlinger K, Rideout III W, Yanagimachi R, Jaenisch R (2000) X-chromosome inactivation in cloned mouse embryos. *Science* **290**: 1578–1581
- Gunster MJ, Satijn DP, Hamer KM, den Blaauwen JL, de Bruijn D, Alkema MJ, van Lohuizen M, van Driel R, Otte AP (1997) Identification and characterization of interactions between the vertebrate polycomb-group protein BMI1 and human homologs of polyhomeotic. *Mol Cell Biol* **17**: 2326–2335
- Gurdon JB, Laskey RA, Reeves OR (1975) The developmental capacity of nuclei transplanted from keratinized skin cells of adult frogs. *J Embryol Exp Morphol* **34**: 93–112
- Hadjantonakis AK, Gertsenstein M, Ikawa M, Okabe M, Nagy A (1998) Generating green fluorescent mice by germline transmission of green fluorescent ES cells. *Mech Dev* **76**: 79–90
- Hahm K, Cobb BS, McCarty AS, Brown KE, Klug CA, Lee R, Akashi K, Weissman IL, Fisher AG, Smale ST (1998) Helios, a T cell-restricted Ikaros family member that quantitatively associates with Ikaros at centromeric heterochromatin. *Genes Dev* **12**: 782–796
- Hahm K, Ernst P, Lo K, Kim GS, Turck C, Smale ST (1994) The lymphoid transcription factor LyF-1 is encoded by specific, alternatively spliced mRNAs derived from the Ikaros gene. *Mol Cell Biol* **14**: 7111–7123
- Hoffmann R, Seidl T, Neeb M, Rolink A, Melchers F (2002) Changes in gene expression profiles in developing B cells of murine bone marrow. *Genome Res* **12**: 98–111
- Huesmann M, Scott B, Kisielow P, von Boehmer H (1991) Kinetics and efficacy of positive selection in the thymus of normal and T cell receptor transgenic mice. *Cell* **66**: 533–540
- Janicki SM, Tsukamoto T, Salghetti SE, Tansey WP, Sachidanandam R, Prasanth KV, Ried T, Shav-Tal Y, Bertrand E, Singer RH, Spector DL (2004) From silencing to gene expression: real-time analysis in single cells. *Cell* **116**: 683–698
- Jenuwein T, Allis CD (2001) Translating the histone code. *Science* **293**: 1074–1080
- Kennison JA (1995) The Polycomb and trithorax group proteins of *Drosophila*: trans-regulators of homeotic gene function. *Annu Rev Genet* **29**: 289–303
- Kikyo N, Wolffe AP (2000) Reprogramming nuclei: insights from cloning, nuclear transfer and heterokaryons. *J Cell Sci* **113** (Part 1): 11–20
- Kim J, Sif S, Jones B, Jackson A, Koipally J, Heller E, Winandy S, Viel A, Sawyer A, Ikeda T, Kingston R, Georgopoulos K (1999) Ikaros DNA-binding proteins direct formation of chromatin remodeling complexes in lymphocytes. *Immunity* **10**: 345–355
- Kurdistani SK, Tavazoie S, Grunstein M (2004) Mapping global histone acetylation patterns to gene expression. *Cell* **117**: 721–733
- Lachner M, O'Carroll D, Rea S, Mechtler K, Jenuwein T (2001) Methylation of histone H3 lysine 9 creates a binding site for HP1 proteins. *Nature* **410**: 116–120
- Lennox RW, Cohen LH (1988) The production of tissue-specific histone complements during development. *Biochem Cell Biol* **66**: 636–649
- Modlinski JA (1978) Transfer of embryonic nuclei to fertilised mouse eggs and development of tetraploid blastocysts. *Nature* **273**: 466–467
- Mutskov V, Felsenfeld G (2004) Silencing of transgene transcription precedes methylation of promoter DNA and histone H3 lysine 9. *EMBO J* **23**: 138–149
- Noma K, Allis CD, Grewal SI (2001) Transitions in distinct histone H3 methylation patterns at the heterochromatin domain boundaries. *Science* **293**: 1150–1155
- Perez-Burgos L, Peters AH, Opravil S, Kauer M, Mechtler K, Jenuwein T (2004) Generation and characterization of methyl-lysine histone antibodies. *Methods Enzymol* **376**: 234–254
- Peters AH, Kubicek S, Mechtler K, O'Sullivan RJ, Derijck AA, Perez-Burgos L, Kohlmaier A, Opravil S, Tachibana M, Shinkai Y, Martens JH, Jenuwein T (2003) Partitioning and plasticity of repressive histone methylation states in mammalian chromatin. *Mol Cell* **12**: 1577–1589
- Peters AH, O'Carroll D, Scherthan H, Mechtler K, Sauer S, Schofer C, Weipoltshammer K, Pagani M, Lachner M, Kohlmaier A, Opravil S, Doyle M, Sibilia M, Jenuwein T (2001) Loss of the Suv39h histone methyltransferases impairs mammalian heterochromatin and genome stability. *Cell* **107**: 323–337
- Pina B, Suau P (1987) Changes in histones H2A and H3 variant composition in differentiating and mature rat brain cortical neurons. *Dev Biol* **123**: 51–58
- Ratcliffe MJ, Julius MH (1982) H-2-restricted T-B cell interactions involved in polyspecific B cell responses mediated by soluble antigen. *Eur J Immunol* **12**: 634–641
- Rice JC, Allis CD (2001) Histone methylation versus histone acetylation: new insights into epigenetic regulation. *Curr Opin Cell Biol* **13**: 263–273
- Schreiber SL, Bernstein BE (2002) Signaling network model of chromatin. *Cell* **111**: 771–778
- Seglen PO (1976) Preparation of isolated rat liver cells. In *Methods in Cell Biology*, Prescott, DM (ed) Vol 13, pp 29–83. New York: Academic Press
- Sewalt RG, van der Vlag J, Gunster MJ, Hamer KM, den Blaauwen JL, Satijn DP, Hendrix T, van Driel R, Otte AP (1998) Characterization of interactions between the mammalian polycomb-group proteins Enx1/EZH2 and EED suggests the existence of different mammalian polycomb-group protein complexes. *Mol Cell Biol* **18**: 3586–3595
- Simon JA, Tamkun JW (2002) Programming off and on states in chromatin: mechanisms of Polycomb and trithorax group complexes. *Curr Opin Genet Dev* **12**: 210–218
- Strahl BD, Ohba R, Cook RG, Allis CD (1999) Methylation of histone H3 at lysine 4 is highly conserved and correlates with transcriptionally active nuclei in *Tetrahymena*. *Proc Natl Acad Sci USA* **96**: 14967–14972
- Su RC, Brown KE, Saaber S, Fisher AG, Merckenschlager M, Smale ST (2004) Dynamic assembly of silent chromatin during thymocyte maturation. *Nat Genet* **36**: 502–506
- Turner BM (2000) Histone acetylation and an epigenetic code. *BioEssays* **22**: 836–845
- Turner BM, Birley AJ, Lavender J (1992) Histone H4 isoforms acetylated at specific lysine residues define individual chromosomes and chromatin domains in *Drosophila* polytene nuclei. *Cell* **69**: 375–384
- van der Lugt NM, Domen J, Linders K, van Roon M, Robanus-Maandag E, te Riele H, van der Valk M, Deschamps J, Sofroniew M, van Lohuizen M (1994) Posterior transformation, neurological abnormalities, and severe hematopoietic defects in mice with a targeted deletion of the bmi-1 proto-oncogene. *Genes Dev* **8**: 757–769
- van der Vlag J, Otte AP (1999) Transcriptional repression mediated by the human polycomb-group protein EED involves histone deacetylation. *Nat Genet* **23**: 474–478
- Wakayama T, Perry AC, Zuccotti M, Johnson KR, Yanagimachi R (1998) Full-term development of mice from enucleated oocytes injected with cumulus cell nuclei. *Nature* **394**: 369–374
- Wilmot I, Schnieke AE, McWhir J, Kind AJ, Campbell KH (1997) Viable offspring derived from fetal and adult mammalian cells. *Nature* **385**: 810–813
- Wreggett KA, Hill F, James PS, Hutchings A, Butcher GW, Singh PB (1994) A mammalian homologue of *Drosophila* heterochromatin protein 1 (HP1) is a component of constitutive heterochromatin. *Cytogenet Cell Genet* **66**: 99–103

- Wu RS, Tsai S, Bonner WM (1982) Patterns of histone variant synthesis can distinguish G0 from G1 cells. *Cell* **31**: 367–374
- Wu RS, Tsai S, Bonner WM (1983) Changes in histone H3 composition and synthesis pattern during lymphocyte activation. *Biochemistry* **22**: 3868–3873
- Yanagimachi R (2002) Cloning: experience from the mouse and other animals. *Mol Cell Endocrinol* **187**: 241–248
- Yang L, Xia L, Wu DY, Wang H, Chansky HA, Schubach WH, Hickstein DD, Zhang Y (2002) Molecular cloning of ESET, a novel histone H3-specific methyltransferase that interacts with ERG transcription factor. *Oncogene* **21**: 148–152
- Zhang Y, Reinberg D (2001) Transcription regulation by histone methylation: interplay between different covalent modifications of the core histone tails. *Genes Dev* **15**: 2343–2360
- Zhao K, Wang W, Rando OJ, Xue Y, Swiderek K, Kuo A, Crabtree GR (1998) Rapid and phosphoinositol-dependent binding of the SWI/SNF-like BAF complex to chromatin after T lymphocyte receptor signaling. *Cell* **95**: 625–636